https://doi.org/10.1016/j.cities.2019.102585

Analysing the effects for different scenarios on surrounding environment in a high-density city

Jian Guo [a], Bingxia Sun [a], Zhe Qin [a], Man Sing Wong [b], Siu Wai Wong [a], Chi Wai Yeung [a], Hao Wang [c], Sawaid ABBA [b], Geoffrey Qiping Shen [a*]

[a] Department of Building and Real Estate, The Hong Kong Polytechnic University, Hong Kong
[b] Department of Land Surveying and Geo-informatics, The Hong Kong Polytechnic University, Hong Kong
[c] School of Management Science and Engineering, Central University of Finance and Economics, Beijing

ABSTRACT

With the development of global urbanization, high-densefity cities faces enormous challenges on land supply. Hong Kong is a megacity with a long-term lack of land and housing supply. To increase the development intensity of built-up areas in Hong Kong, a minor relaxation of plot ratio/building height (PR/BH) restrictions for twenty-one sites in the three target study areas of Kai Tak Development Area (KTDA) has been approved by the Town Planning Board in 2015. This research project aims at providing scientific evidence on the impact of this relaxation and possible further relaxations using 3D spatial analysis and simulation technologies. After a 3D model of Kai Tak and surrounding areas being generated, effects of increased PR/BH on skyline, visibility, shadow and insolation, air temperature, and wind ventilation of the three study were successfully simulated and analysed in terms of five scenarios. Research findings indicated that, except the extreme case of Scenario 5, no significant changes were found in Scenario 2, Scenario 3 and Scenario 4 when compared with the original plan of Scenario 1. More importantly, in comparison with the approved proposal by the Town Planning Board, gross floor areas for domestic uses and non-domestic uses were estimated to increase 156,200 m^2 and 119,900 m^2 respectively, which would offer 2,603 additional residential units and 9,110 potential residents. As a pilot study focusing on the KTDA in Hong Kong, this project may also serve to provide new methodological and theoretical insights to facilitate rational discussion and debate on changing land development density in other similar hyper-dense cities.

Keywords: Spatial analysis, Computational fluid dynamics, Simulation, Building regulations and controls, High-density city

1. Introduction

In recent decades, we have witnessed the rapid development of global urbanization and the rise of many super cities, such as New York, Tokyo, and Hong Kong. The development of global urbanization has accumulated enormous wealth for us, brought more opportunities, changed people's way of life, and improved quality of life and environment. According to the report published by United Nations New York (Nations, U., 2014), the urban population will be increased by 2.5 billion by 2050, with nearly 90% of the increase presented in Asia and Africa. At the same time, the proportion of the world's population living in cities is expected to increase, reaching 66% by 2050. Therefore, global urbanization also brings a series of negative influences, such as environmental problems, traffic conditions, housing tensions, employment pressure, and social

problems. Among them, environmental issues are closely related to human's health, such as air pollution, air blockage, heat island effect, and ecological environment destruction. A good urban planning can effectively reduce the negative effects brought about by reducing the heat island effect and promoting air circulation while satisfying the urban space utilization rate.

Hong Kong is a typical megacity. It is one of the most densely populated cities in the world, with a very high density of buildings, while Hong Kong is a mountainous region, leaving limitation for the expansion of this city. Because there is very rare land available in Hong Kong, land use issues may be the single most important challenge facing the Hong Kong Special Administrative Region (HKSAR) government (Shen et al., 2009). Therefore, it is particularly important to improve the urban space utilization in Hong Kong. To raise housing supply, the HKSAR government has increased development density in some key development areas, e.g. Kai Tak Development Area (KTDA). Hong Kong's development intensity is mainly controlled by building (planning) regulations, lease conditions, and statutory outline zoning plans. These factors inevitably impose restrictions on plot ratio (a ratio between the gross floor area of a building and the area of the site on which it is erected), site coverage, and building height of each land lot. To achieve efficient and sustainable usage of the scare land in Hong Kong, elevating the development intensity of built up areas through minor relaxation of plot ratio/building height (PR/BH) restrictions is a choice to raise land provision in a short time. Therefore, the Civil Engineering and Development Department (CEDD) suggested minor relaxation of maximum PR/BH restrictions for the twenty-one target sites in 2015 (CEDD, 2015).

This study takes Hong Kong as an example to study how to improve the urban space utilization while avoiding or minimizing the brought negative effects. This research aims to create the a 3D model of the areas which are still under constructions in Kai Tak Development Area (KTDA) and the areas nearby through gathering and integrating associated data. Based on the 3D model, various 3D spatial analyses and comparisons were executed for five different PR/BH scenarios, including skyline, visibility, shadow and insolation, air temperature and wind ventilation. The vivid findings of this study can make decision makers formulate scientific and rational decisions for the sustainable urban development. Based on the experimental results, it can be proved that this approach can also be applied to other densely populated cities around the world.

2. Literature review

This section reviews the literature on how to increase the development intensity and support decision-making processes using 3D GIS technology. Finally, the literature review on air temperature and wind ventilation simulation is presented.

Generally, development intensity is investigated by Environmental Impact Assessment (EIA), exploring the carrying capacity of infrastructure, and by conducting public consultations in certain sites as well (Environmental Protection Department, 1997; Maunsell AECOM, 2006). An EIA typically includes a prediction and assessment of a series of environmental consequences including noise pollution, impact on air, soil and water, waste management, visual and landscape impact caused by the proposed development. In addition, assessment of carrying capacity concerning basic infrastructure provisions, such as transportation, communication, sewage, water and electric systems, play important roles in the land-use decision making process (Joardar, 1998). Public engagement also guides decision makers on urban planning in Hong Kong (CEDD, 2008). In this context, to explore the feasibility of a minor increase of the development intensity for the twenty-one sites in KTDA, CEDD has conducted various reviews and assessments with respect to the carrying capacity of environment and infrastructure (CEDD, 2015).

However, these previous reviews and evaluations are mainly implemented based on 2D geographic information system (GIS). As most people may not visualize the effects of relaxed PR/BH restrictions from a static 2D image, a dynamic 3D visualization is needed to help people better understand the real world. This study measures the effects of a minor increase of PR/BH on twenty-one sites in the KTDA by virtue of 3D GIS and spatial analyses of urban skyline, visual effects of mountain ridgeline, shadow and insolation, air temperature, and wind ventilation. Five scenarios in terms of different PR/BH restrictions for the three study areas are created and compared to help decision makers formulate effective and farsighted decisions.

At present, 2D GIS has been widely adopted in urban construction and development control. However, 2D GIS is not sufficient for rapid urban development, while advanced 3D GIS is integrated with 2D GIS to convey complicated geographic phenomena. The fast developing3D GIS technologies have been increasingly applied in the decision-making process for urban development. For instance, the feasibility of 3D virtual reality for participatory planning was first investigated by Ranzinger and Gleixner (1997) and Pullar and Tidey (2001). They examined the feasibility of using 3D visualization techniques and a structured evaluation approach (Delphi) to facilitate visual impact assessment and supporting decision-making. The experimental results indicated that 3D visualization techniques can support the process of urban and landscape planning. However, the results are still far from the goal of enabling data communication and visualization among groups. Geertman (2002) and Hudson-Smith et al. (2005) built a series of technologies based on the idea of a "virtual city" to disseminate planning information and support participatory planning. Zhang et al. (2004) analysed urban development issues by 3D modelling and spatial analyses in terms of flood, energy, visibility, solar panel and air pollution. In a similar way, Mak et al (2005) utilized 3D GIS to establish and evaluate the city skyline of Hong Kong, which demonstrated that 3D GIS can effectively visualize and practice the Hong Kong urban design guidelines. Significantly, Petti et al. (2006) conducted an evaluation of the effectiveness of 3D visualization technologies, with the results showing that while professional planners are comfortable with low-level visual specificity, people who only have basic computer skills are more comfortable with mid-level visual specificity. Stevens et al. (2007) took a step further to introduce the simulation of urban growth based on cellular automation (CA) in a 3D environment. A growing number of researchers have therefore concentrated on applying 3D visualization/virtual reality technologies to urban planning, e.g., Foth et al. (2009), Chen et al. (2011), Isaacs et al. (2011), Xu and Coors (2012), and Yeo et al. (2013). One of those most worthy of mention is that Guo et al. (2017) who used 3D GIS analysis technology to simulate the environmental impacts based on various 3D models. However, they only focused on the urban skyline, visual impact, and sunlight hours analyses in their most recent study. The 3D models developed for this research go further by including wind ventilation and air temperature, the two most influential factors on people in urban planning.

As a major application to 3D spatial simulation of urban environments, microclimate can be affected by many factors. Air temperature and wind ventilation are two interrelated elements that contribute to microclimate. Croker (1956) found that wind could carry hot air to shaded areas to increase the air temperature in those areas while carrying cool air to exposed areas to reduce air temperature there. Wong et al. (2011) initiated the use of 3D GIS for investigating the "wall effect" of increasing high-rise buildings alongside the coast of Kowloon, Hong Kong. With the increasing density of urban land development, urban canyons are commonly found in many populated urban areas and are characterized by tall buildings. Many researchers have investigated air temperature and ventilation in urban canyons, for these two factors influence heat exchange within an area and

affect human comfort at the pedestrian level in urban canyons (Bottillo et al. 2014). Cai (2012) and Wang et al. (2013) used different simulation methods to analyse air-flow patterns in an urban canyon under heating effect. Air turbulence in street canyons will be strengthened by heat from the sun. Bourbia and Awbi (2004) studied the shading effect of buildings on the ground surface in a street, and investigated the influence of the sun on an urban canyon, as well as the effect on air temperature. They found that solar radiation has more influence on air temperature than on the height to width (H/W) ratio, which is calculated by dividing the average building height by the street width. The shading effect of the buildings becomes increasingly evident as the H/W ratio increases, and it can reduce air temperature in the shaded area. A large H/W ratio implies that a large area of building surface will be exposed to direct solar radiation. Thus, the buildings will then release heat to increase nearby air temperatures. However, Nakamura and Oke (1988) discovered that the heated parts of buildings could only change the air temperature nearby, and the effect is limited as the distance increases from the heated surfaces.

Although many of the studies described above have applied 3D spatial analysis and virtual reality technology to the issues in urban development and microclimate simulation, only a few have focused on the issue of development control. To fill the gap, this study therefore explored the viability of minor increase of PR/BH in a redevelopment area through the simulation of changes to the visual and microenvironment based on 3D models. The research also quantitatively analysed the impacts of the changes on the surrounding residents.

3. Methodology

3.1 Framework

Fig.1 shows the framework with four main steps of this research. Firstly, a Kai Tak 3D model and its surrounding regions was established based on the relevant information from the approved KTOZP and available 3D spatial data and digital elevation model (DEM). Secondly, five various 3D spatial analyses were conducted to evaluate the impacts of different scenarios. The mountain ridgeline analysis was conducted by introducing A DEM into the 3D model. Thirdly, based on five scenarios with various PR/BH, a comparison of various PR/BH scenarios was carried out to assess how the relaxation of PR/BH can bring effects to the surrounding regions and the people in them. To verify preliminary research findings, two focus group meetings were organized to collect advice and comments from professionals, district councillors, and committee members. The findings of the first three steps were refined and consolidated based on their views and suggestions. Finally, the report provides a discussion and conclusion with reference to previous research.

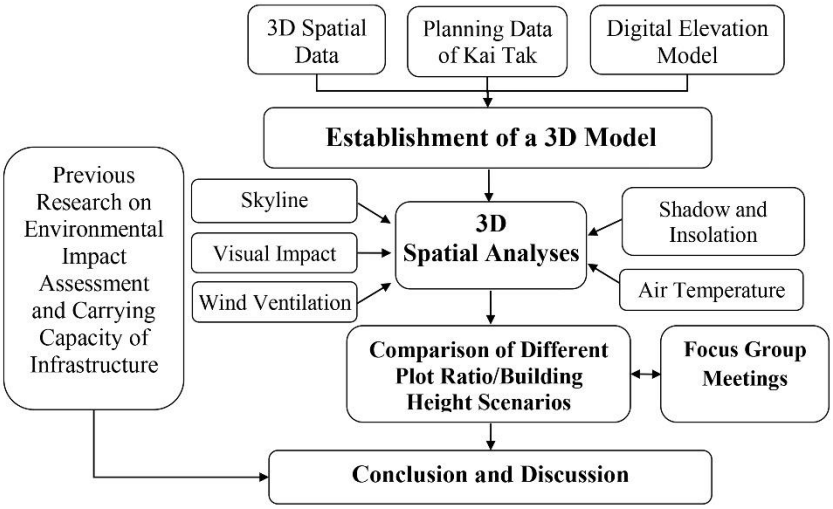

Fig.1. Research framework.

3.2 Study area and data collection

The study area was defined using a DEM, the mountain ridgeline, visual environment, and other factors taken from the EIA ordinance of HKSAR's Environmental Protection Department (Environmental Protection Department, 1997). As shown in Fig.2, the Kai Tak rebuilt planning area is displayed in red, where the twenty-one target sites are distributed as shown in Fig.3. The grey outer line means the boundary of potential affected region within a 500 m radius.

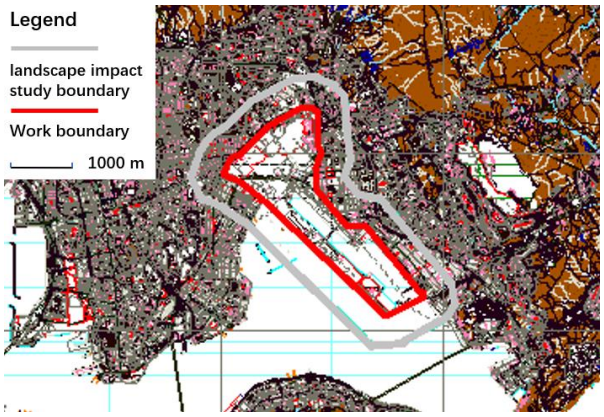

Fig. 2. Study region.

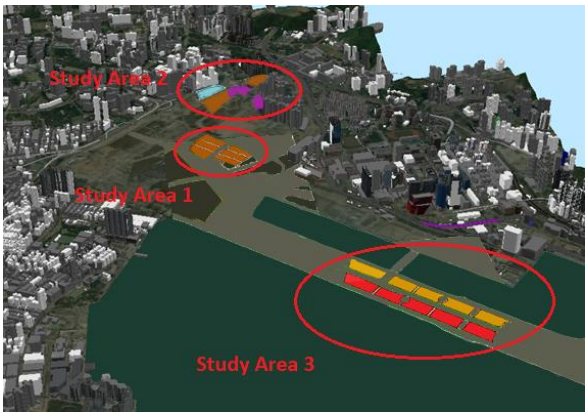

Fig. 3. Target sites in the three study areas.

3.3 3D spatial analysis models generation

The 3D data of surrounding areas and the built-up areas in KTDA are readily available from Lands Department of Hong Kong. For the areas where are still under constructions, the 3D models were designed and generated using the commercial software CityEngine referring to the planning scheme of this study area for the areas without existing 3D data (i.e. KTDA).

The formulation of five hypothetical scenarios was based on an analysis of the development restrictions, such as plot ratio, site coverage, and building height (TPB, 2012; 2015), which were imposed by the Conditions of Sale, the Outline Zoning Plans, and the Building (Planning)

Regulations (Building Department, 2012). The Kai Tak Development Urban Design Guidelines and Manual were taken into consideration to refine the parameters of each scenario further, such as plot ratio, building height, gross floor area (GFA), and site coverage (KTDUDGM, 2015).

Five scenarios with different PR/BH were built for the twenty-one sites in consideration of the aforementioned rules and guidelines. S1 (Scenario 1) is the initial plan with a low plot ratio around 4.5. S2 (Scenario 2) is raised by CEDD and approved by the TPB with a higher plot ration around 5.5. S3 (Scenario 3) and S4 (Scenario 4) refer to the further increase of PR/BH based on S2. The PR/BH of S3 and S4 for this study were determined as follows:

$$S3=S2^{*}\,[1+(S2-S1)/(2\times S1)] \quad (1)$$

$$S4=S2^{*}\,(1+(S2-S1)/S1) \quad (2)$$

Take 1K2 site in study area 1 as an example, Fig. 4 shows that the growth rate between the plot ratio of the initial plan S1 and the approved plan S2 was 22%. Using Formulas (1) and (2), the plot ratio of S3 improved at half of this growth rate of 11% to 6.1, whereas the plot ratio of S4 raised at the same growth rate of 22% to 6.7. To investigate the extent to which the PR/BH restrictions can be relaxed, a critical point of PR/BH should be identified. In this regard, Scenario 5 (S5), which is considered as an extreme case compared with the other scenarios, was added by increasing the growth rate to 42% and the plot ratio to 9.5 (similar plot ratio as Mong Kok, which is the most population density region in Hong Kong) based on S4. It is worth noting that the PR adopted for S5 is much higher than others. The main purpose of a high growth rate was to identify a critical point beyond which the proposed development would have significant impacts on the surrounding areas. Based on the increased PR, the building height of each scenario was then calculated. In the calculation of building height, various storey heights adopted for different types of building were as follows: 3.2 m/floor for R(B) (residential group B, medium density development); 3.5 m/floor for R(C) (residential group C, low density development); 4.5 m/floor for C (commercial); and 4.0 m/floor for G/IC (government, institution or community). In this way, the site coverage and GFA/floor in each scenario can be acquired. Table 1 shows the models generation rules of the five scenarios for each site in study area 1.

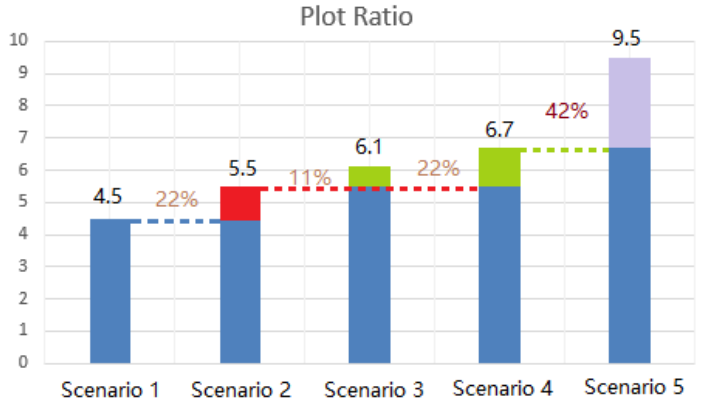

Fig. 4. Calculation of plot ratio under different scenarios (e.g. site 1k1).

Table 1
Models generation rules of the five scenarios for each site in study area 1.

Study area 1	1K1	1K2	1K3	1L1	1L2	1L3
Zone	R(B)2	R(B)2	R(B)2	R(B)2	R(B)2	R(B)3
Site area (m^2)	9,719	9,699	11,263	7,317	9,482	8,803
Kai Tak OZP						
Max. PR	4.5	4.5	4.5	4.5	4.5	3.5
Max. Site coverage	40%	40%	40%	40%	40%	44%
Max. BH (m)	110	110	110	100	100	50/100
BPR						
Max. PR	9.0	9.0	9.0	9.0	9.0	7.5/10.0
Max. Site coverage	37.5%	37.5%	37.5%	37.5%	37.5%	42%/40%
S1 (original)						
PR	4.5	4.5	4.5	4.5	4.5	3.5
BH (m)	110	110	110	100	100	50/110
S2 (approved)						
PR	5.5	5.5	5.4	5.4	5.4	4.2
BH (m)	130	130	130	120	120	50/120
S3 (increased)						
PR	6.1	6.1	5.9	5.9	5.9	4.6
BH (m)	140	140	140	130	130	60/130
S4 (further increased)						
PR	6.7	6.7	6.5	6.5	6.5	5.0
BH (m)	150	150	150	140	140	60/140
S5 (extreme case)						
PR	9.5	9.5	9.2	9.2	9.2	7.1
BH (m)	210	210	210	180	180	85/180

Based on the models generation rules shown in Table 1 above, 3D buildings of twenty-one target sites in the KTDA can be established. Fig. 5 shows the buildings of five scenarios built for study area 1 in yellow. A smooth transition of building mass from towers to low blocks can be observed. The site coverage and building height in each scenario were slightly changed. Moreover, Fig. 6 provides a set of pictures showing the integration of 3D models of Kai Tak with their surroundings.

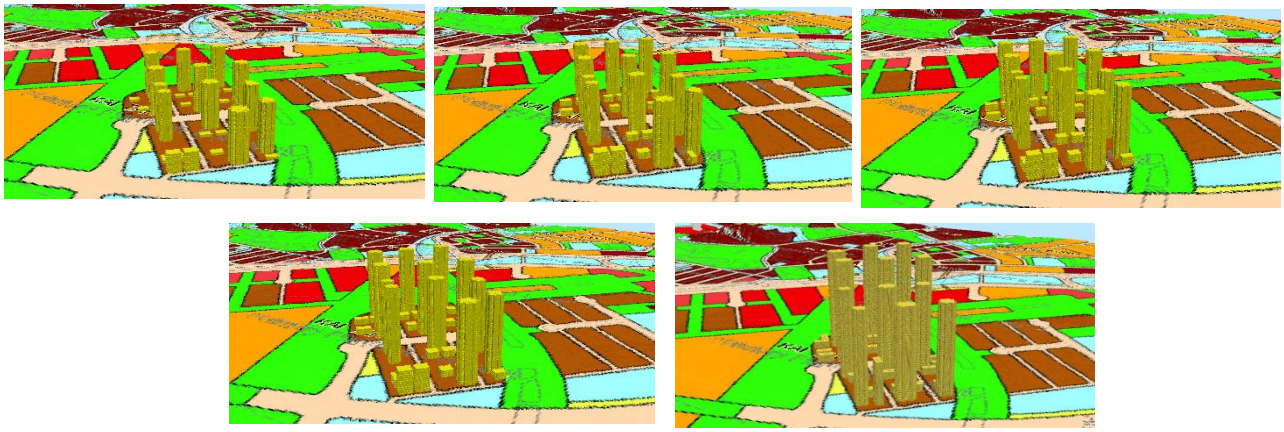

Fig. 5. Five scenarios in study area 1.

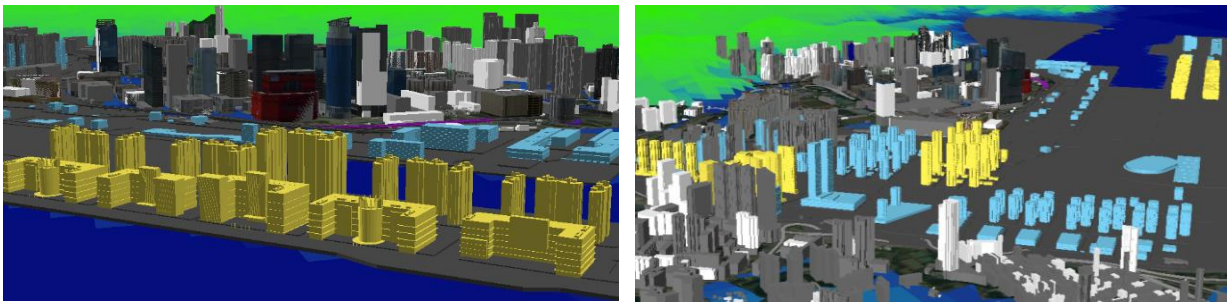

Fig. 6. 3D models of the Kai Tak and the areas nearby.

3.4 Computed Fluid Dynamics models generation and setting

The relative comparisons of changes in air temperature and wind ventilation in the five different scenarios were carried out by simulating microclimate using the ENVI-met software. The ENVI-met simulates microclimate by incorporating 3D building and other spatial data into a 3-dimensional Computed Fluid Dynamics (CFD) model. This model has been widely used and validated in several applications for prediction of spatial patterns of microclimate conditions in various and urban and non-urban environment. For example, Xun et al. (2014) applied ENVI-met model to simulate urban microclimate in Chongqing, China. They have used this microclimate information for a comprehensive evaluation of pedestrian-height wind environment and thermal comfort and provided recommendations to improve the design of urban environments. Likewise, Morakinyo and Lam (2016) used ENVI-met simulations for studying the effect of different types of urban greening patterns on the microclimate conditions in urban canyons. Maggiotto et al. (2014) made use of ENVI-met to study the issue of urban heat islands in Lecce, Italy, and found that the ENVI-met can accurately present the change in temperature throughout a day. Shahidan et al. (2012) evaluated cooling effect by combination of trees and ground materials with outdoor and building environment by using and validated microclimate simulations in Putrajaya, Malaysia. Furthermore, Ng et al. (2012) applied and validate ENVI-met simulations to study cooling effect of greening in high-density urban landscape of Hong Kong. Therefore, considering the wide scale acceptance and applications of the model for simulating microclimate conditions in urban areas, this study used numerical simulation model of ENVI-met to analyse the spatial changes in air temperature and wind ventilation conditions due five different building models.

To simulate the microclimate by ENVI-met, some assumptions were made, including the steady temperature and no heat storage inside the buildings, and the default setting of soil temperature and humidity. Although these parameters, such as grid size, cell height, thermal storage in buildings, soil temperature and humidity etc., are of utmost importance for absolute urban microclimate mapping, keeping these parameters constant will be served as controlling parameters to conduct comparative analysis of microclimate under different scenarios of spatial arrangements of buildings. Regions for analysis were determined during early stage followed by modelling of three study areas and their surrounding areas in the ENVI-met. The 3D building models were developed by allocating height values to building's footprints. The vertical grids are generated by the equidistant method, and the vertical grids are the same except for the bottom. Five scenarios were established for analysing air temperature and wind ventilation. Initial weather information for a particular date and time were acquired from the Hong Kong Observatory and are listed in Table 2 below.

Table 2
Configuration settings in ENVI-met.

Figures	4 August 2014 (Summer)	5 February 2014 (Winter)
Simulation start time	7:00 a.m.	7:00 a.m.
Total simulation hours	24	24
Wind speed at 10 m above ground (m/s)	1.5	4.5
Wind direction	Southeast	East
Initial atmosphere temperature (deg. C)	29.5 (Study area 1 and 2) / 29 (Study area 3)	15.5
Specific humidity at 2500 m (g Water/kg air)	6.77	9.74
Relative humidity at 2 m (%)	91.5	83

The dates of August 4, 2014 and February 5, 2014 were chosen in this study. The air temperatures during these two selected days were 29.5 °C (29 °C for the area near the harbor) and 15.5 °C respectively, as shown in Table 3. These temperatures are nearly the same as the mean air temperatures in February and August 2014. Therefore, to a certain extent, these two days can represent Hong Kong's normal weather condition in summer and winter. In addition, the meteorological data of study areas 1, 2, and 3 were obtained from several nearby observation stations. In this configuration setting, a total of 24 hours were assigned for the whole simulation process.

Table 3
Mean air temperature in 2014 observed in the Hong Kong Observatory (HKO, 2015).

Month	January	February	March	April	May	June	July	August	September	October	November	December
Mean (°C)	16.3	15.5	18.7	22.6	26.4	29.0	29.8	29.0	29.0	26.2	22.6	16.3

Finally, the comparison images of air temperature and wind ventilation of S2 versus S3, S2 versus S4, and S2 versus S5 were produced from the simulation outputs using the post-processing ENVI-met software. In the comparative maps, the air temperature and wind simulation results of S2 was used as a reference, while, S3, S4, and S5 functioned as observations. Thus, the comparison values can be calculated by deducting the reference value from the observation value. In this study, the bottom grid (z=0) with a height of 1.5 m was selected, as air temperature and wind speed has significant impacts at ground level.

4. 3D spatial analysis and experimental results

4.1 Urban skyline analysis

Since no two skylines are alike, the city skyline can be used as a representative and identification of a city. Two urban skylines were created to present the profiles of the three study areas. A comparison among the five scenarios with different PR/BH shows that to what extent the increased PR/BH brings effects to the city profiles.

Taking Skyline 1 as an example, it was mainly used to represent the land and buildings in study areas 1 and 2. The yellow buildings are the buildings from study areas 1 and 2, and the grey ones

are the surrounding buildings. Heights of the yellow architectures in study areas 1 and 2 gradually improved from S1 to S5, shown in Fig.7. However, the growth PR/BH brings insignificant influence on the sight of Skyline 1. Similarly, Skyline 2 mainly represents the land and buildings in study area 3. Heights of the buildings are also gradually increased from S1 to S5. Similar to Skyline 1, the negative effect of increasing PR/BH for Skyline 2 is insignificant. For both the residents nearby and the travellers who sense the change of the skyline from S2 to S4, there are no significant visual changes. Therefore, S4 is the recommended scenario for the urban skyline analysis. Compared to the traditional method, 3D GIS offers a more clear and active method to present the profiles of an urban by its skylines.

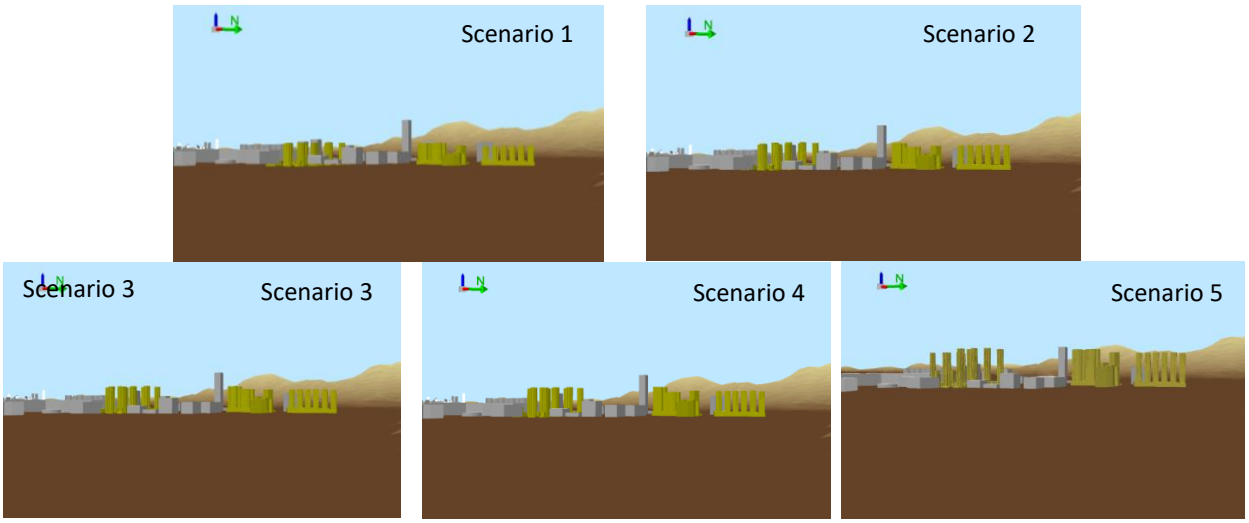

Fig. 7. Scenes of Skyline 1.

4.2 Visual impact on mountain ridgeline analysis

The urban design guidelines (Planning Department and RMUM Hong Kong Limited, 2002) indicate that the mountain ridgelines are very valuable to the high-density city centre (like Kowloon island), which were presented in a red line in Fig.8. Therefore, protecting mountain ridgelines is a considerable concern that draws particular attention in city redevelopment. The long-term aim is to elevate Hong Kong as a one of the top cities in the world through improving the quality of its built environment. Therefore, the conservation of ridgelines should be considered as much as possible in urban development/redevelopment.

Seven vantage points along the Victoria Harbor serving as starting reference points for considering the sights to mountain ridgelines in Hong Kong. Because the study areas are located in Kowloon island, only the opposite three vantage points in Hong Kong Island were chosen. Subsequently, view corridors from the three vantage points were generated to protect sights to the mountain ridgeline in Kowloon area.

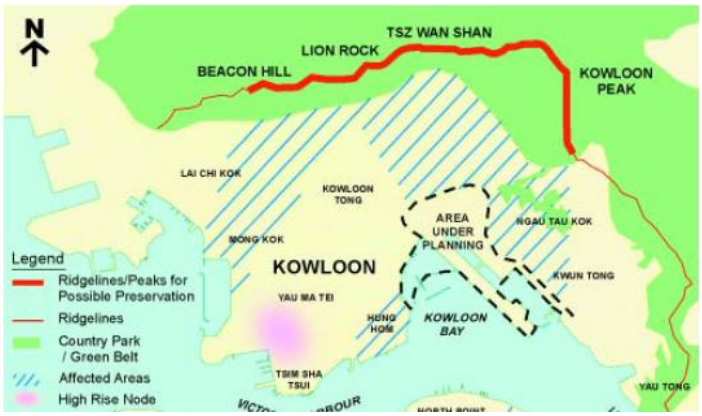

Fig. 8. Ridgelines on Kowloon Island

To conserve valuable ridgelines in Hong Kong, the building free zone (twenty percent of the mountain height to the top) was suggested for maintenance during the urban redevelopment according to the Metroplan guidelines (Planning Department, 2015). The line along the bottom of the building fee zone is called limit of the roofline. To follow this suggestion, several 1° interval sampling points were determined along the limit of the roofline of the mountains in Kowloon area. View corridors starting from the three aforementioned vantage points to the sampling points at the limit of the roofline were generated to define the visual impact on the ridgeline based on five scenarios, which is shown in Fig.9. There is no sightline was blocked for S2, S3, and even S4, which implied that no effect on the visibility under these three scenarios. However, one sightline was blocked in S5 at the Quarry Bay Park vantage point, as shown by the red sightline in Fig.10.

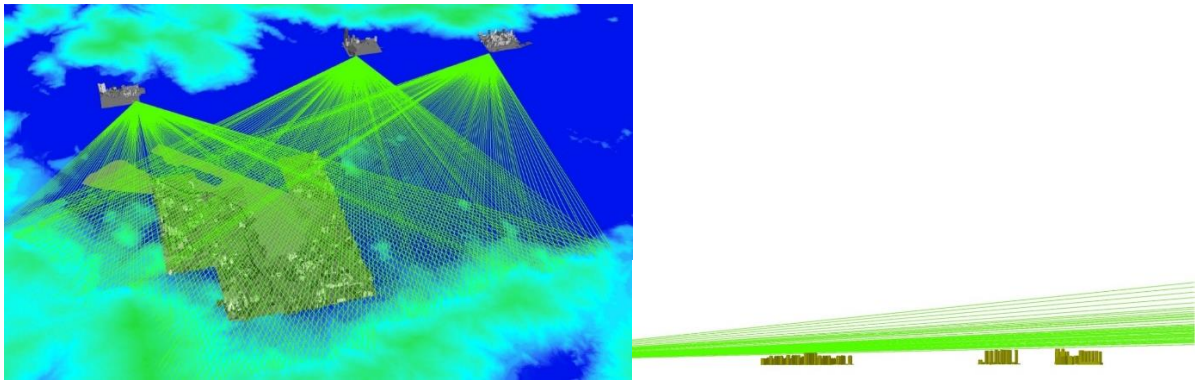

(a) All the visible sightlines. (b) Profile of all sightlines.

Fig. 9. Visible sightlines for S2, S3, and S4.

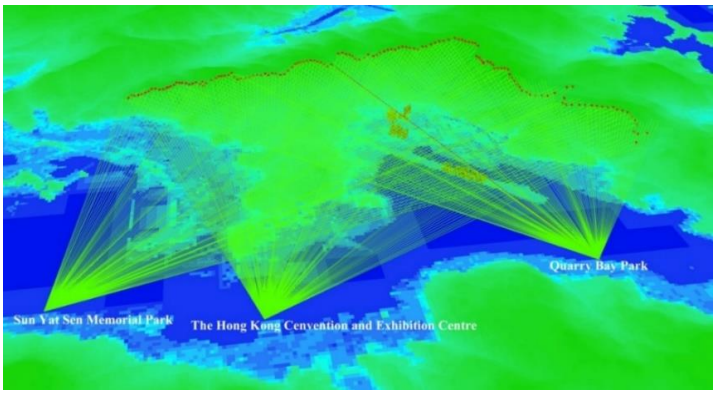

Fig. 10. All sightlines at the three vantage points in S5.

For the blocked sightline from the vantage point located at Quarry Bay Park in S5, the sightline angles and block percentage were calculated and are shown in Fig.11. The block percentage is only 1.23%, which indicates that there is very slight influence on the protection of mountain ridgelines even under an extreme condition. Therefore, increasing the PR/BH of the target twenty-one sites brings a minor negative impact on the visual impact of mountain ridgeline for Hong Kong residents and tourists. S4 is also recommended as the most suitable scenario for the visual impact on mountain ridgeline analysis.

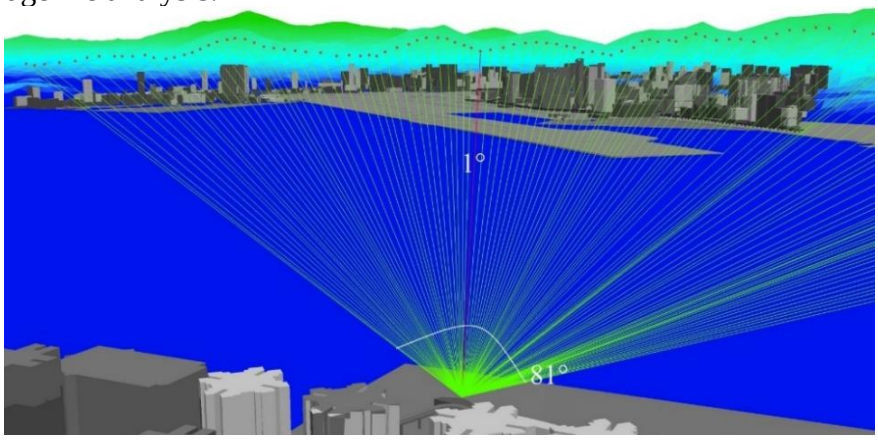

Fig. 11. Angle of sightlines in S5.

4.3 Shadow and insolation analysis

Shadow and insolation are generally two important factors of environmental assessment for urban planning. A shadow is a dark area where sunlight is blocked via an opaque object (Shadow, 2019). Insolation is the solar radiation that arrived at the surface of the earth (Insolation, 2018). In general, insolation can be used to calculate the allocation of sunlight duration in a designated region.

The effect of insolation and the allocation of sunshine with minor relaxation of PR/BH through the comparison of S3 to S2, S4 to S2, and S5 to S2 were investigated. Based on the solar azimuth and altitude presented in Fig. 12, six regions were determined for the analysis (three red regions for summer and three blue regions for winter). The large difference between sunlight intensity and illumination time is considerable; hence, both winter and summer were examined in the study. Finally, the average sunlight hours per day of the six regions were calculated and related locations were determined. All the parameters for the calculation are provided in Table 4, which include solar azimuth and altitude for determining the time of sunrise and sunset.

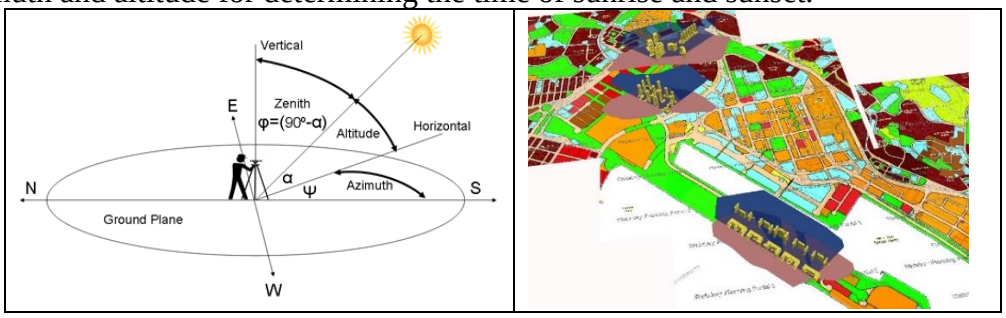

Fig. 12. Illustration of solar azimuth and altitude, and six analysis regions.

Table 4
Parameters for insolation calculation.

Sun (KTDA)	Winter	Summer
Azimuth	127°SE-232°SW	72°ENE-288°WNW
Altitude	20°	20°
Time	8:40 – 16:00	7:15 – 17:32

The findings were showed in a 3D environment within the three study areas for analysis both in summer and winter. Due to the high insolation effect, take the summer findings as an example only. The average sunlight hours for a particular day in summer were measured for the selected study regions. Fig. 13 illustrates ten categories of sunlight hours in summer ranging from (0, 1] to (9, 10] in various colored facades of the buildings and varied areas of the ground. The findings reveal that the discrepancies between S3 to S2, and S4 to SS are unobvious, when visually comparing the colored areas. It is clear that more (green, yellow and blue) areas in S5 are having a shadow affect and obtaining less exposure to the sunlight in summer. Correspondingly, fewer (red) areas in S5 experience the summer sunlight for a long exposure (9-10 hours). Similar results were acquired in winter.

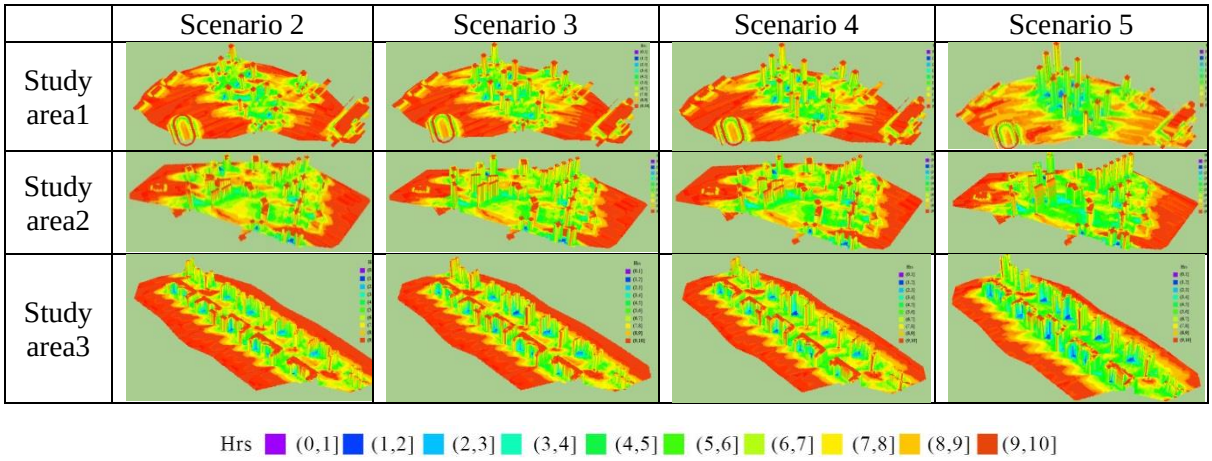

Fig. 13. Results of average sunlight hours per day in summer.

A quantitative analysis was conducted to obtain accurate statistics for the three study areas in summer. According to Fig.14, the area sizes shown on the left legend, and relevant percentage of architecture facades and floor for each classification of sunshine hours were quantified. The bar charts presented that the area percentage shown on the right legend decreases at the longest sunlight categories (9-10 hours) as a result of the raised PR/BH, while other shorter sunlight classifications increase accordingly. A similar quantitative analysis was carried out in winter. The trends of differences for study areas 1, 2, and 3 are similar.

To further check the change trend of insolation under various scenarios, the discrepancies in area size and corresponding percentage among S3 to S2, S4 to S2, and S5 to S2 were computed and illustrated by the blue, red, and green curves, respectively. As shown in Fig.14, the variation rate of the three different curves are presented on the right legend. The extent of the variations for the target three study areas is comparatively small except the extreme case (within 5% for S2 versus S3, within 7% for S2 versus S4, and within 20% in the extreme case of S2 versus S5). The three curves demonstrate that the difference in the longest sunlight classification, namely (9, 10] and (8, 9], decreases because of increased building height. However, all the changes are

insignificant except for the extreme case, which demonstrates that the effect of an increase of the PR/BH in summer is insignificant. The similar results were also achieved in winter for study areas 1, 2, and 3. However, the percentage of change in winter is relatively smaller than in summer. What's more, the residents nearby who walk through this community will experience less sunlight exposure especially in summer, which is an extra benefit to the residents after the minor relaxation of the PR/BH.

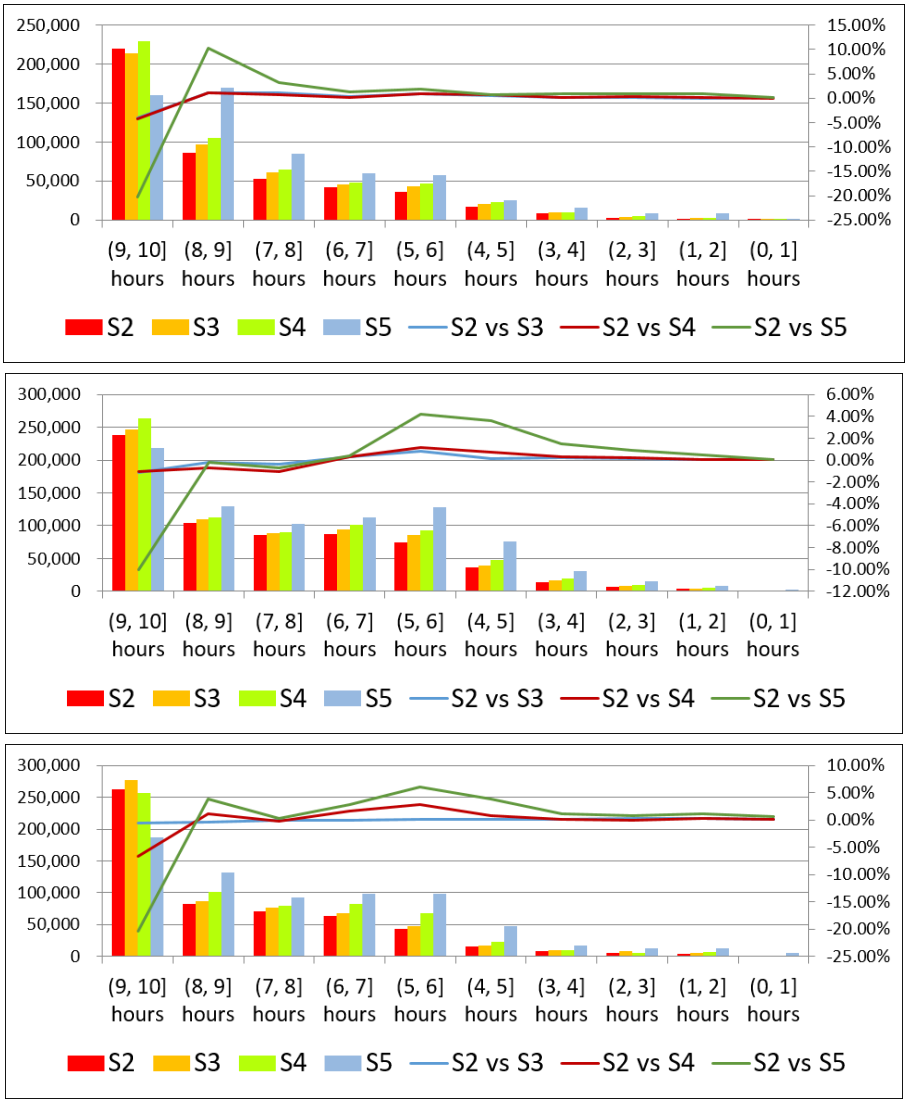

Fig. 14. Comparison of insolation and areas in summer.

4.4 Air temperature analysis

To present the increase in building heights in terms of air temperature, a color legend was designed to identify the changes. The simulation results at both 1 am and 1 pm (local time) were extracted and are displayed in Fig.15. According to the legend, the air temperature ranged from −0.20 °C to 0.20 °C listed as white is explained as a negligible variation. Air temperature beyonds this range (below −0.20 °C in green or above 0.20 °C in red) is considered as a significant variation.

Comparing the results both in winter and summer, there is an obvious change in the winter afternoon. Study areas 1 and 2 exhibit an insignificant change in S3 and S4, which indicates an insignificant change in air temperature after increasing the PR/BH of buildings. A significant increase in air temperature was observed in the lower left part of study area 1 in S5 when compared with that in S2 in the winter afternoon.

An evident decrease (over 0.2 °C) in air temperature was observed in study area 3 (S5 versus S2) environments in the winter afternoon. This decrease is probably attributable to the deep canyon around some parts of the area, which is related to its high H/W ratio. The street surface is almost completely shaded for most time of the day so that the air temperature is not easily warmed up by solar radiation. In addition, the warm air above building tops during the afternoon cannot reach the lower part of the canyon since warm air flow from the upper part is skimmed by the deep canyon (Johansson, 2006). Why do significant changes happen in almost the same place for the three scenarios? It is found that the separation between the buildings determines where the changes appear and the sun's position in the winter afternoon determines the direction of the changes. Specifically, the larger separation between the first two (from left to right) buildings located at the second line (from bottom to top) is the main reason why obvious changes happened here; also, the sun is located in the southwest direction in winter afternoons to study area 3. Due to the shadowing effect, most of the significant decreases happened in the northeast direction (the opposite direction to the sun) of the buildings. Conversely, air temperature changes are insignificant both at 1 am and 1 pm in summer according to our findings.

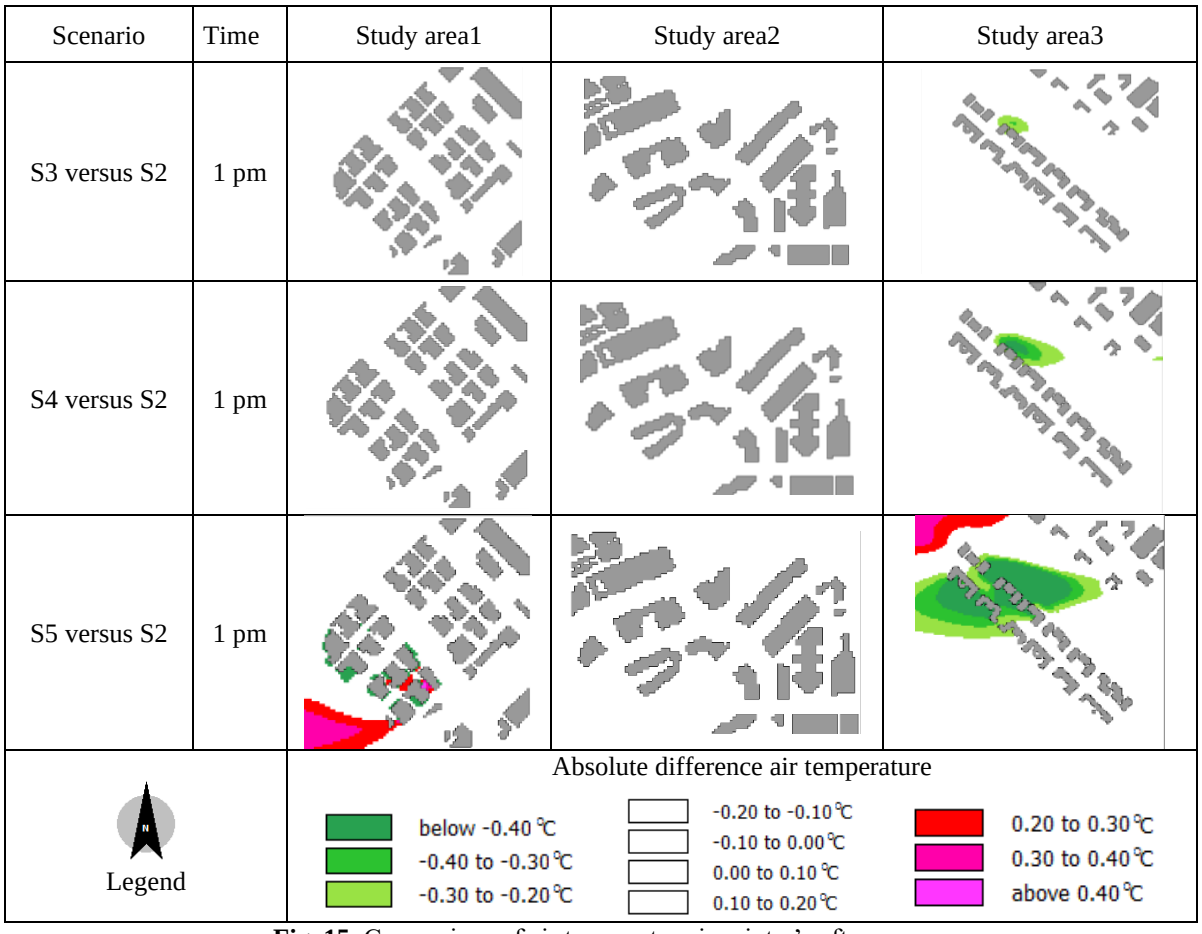

Fig. 15. Comparison of air temperature in winter's afternoon.

4.5 Wind ventilation analysis

Similarly, the discrepancies of wind speed were categorized into various intervals for identification. Based on the subjective reaction to the air motion (Bradshaw, 2006), the minimum wind speed that can be sensed by people is 0.25 m/s, and the wind speed between 0.25 m/s and 0.51 m/s that can be felt by human beings is comfortable. Besides, the wind direction was also simulated and symbolized by arrows in the three study areas, where a long arrow indicates fast wind speed. An east wind was defined to initiate the simulation in this study.

Changes of wind speed are represented using both the legend values and the length of the arrows, as shown in Fig.16. Similarly, changes in terms of wind direction are presented using the arrows' direction. A larger difference in wind speed is evident from the comparison result for study area 2 between S5 and S2 than the other scenario comparisons; a longer wind arrow can be identified. Wind direction may change depending on site conditions, such as the position and distribution of buildings. After the wind flows through the buildings in the three targeted areas, it is shown as being deflected. Slightly increasing development intensity only results in slight changes in both wind speed and direction around the study areas in winter.

When PR/BH increases to an extreme condition (as shown in S5), wind speed and direction change significantly in winter. Study area 1 demonstrates an insignificant change in wind speed in S3 and S4. The change in wind speed in study area 2 in S3 is insignificant, but a significant increase (red area) in wind speed is noted in a small part of study area 2 in S4. In some parts of study area 3, a significant increase in wind speed (approximately 0.3 m/s) is observed near the sites after increasing the heights of buildings in S3. The extent of increased wind speed becomes larger in S4, and the extent of increased wind speed is largest in S5. Meanwhile, a decrease in wind speed can also be observed in study area 3 in S3, S4, and S5. The increase of wind speed may be due to the presence of high-rise buildings leading to greater wind flow at the pedestrian level due to downward directed wind flow below the stagnation point as a results of high rise buildings in windward direction whereas lower height of buildings in the windward direction results in smoother in flow of wind. Similar phenomenon is also observed in another study area in high-density urban landscape of Hong Kong where increases in the building height, across the wind inflow direction, induces increases in wind speed.

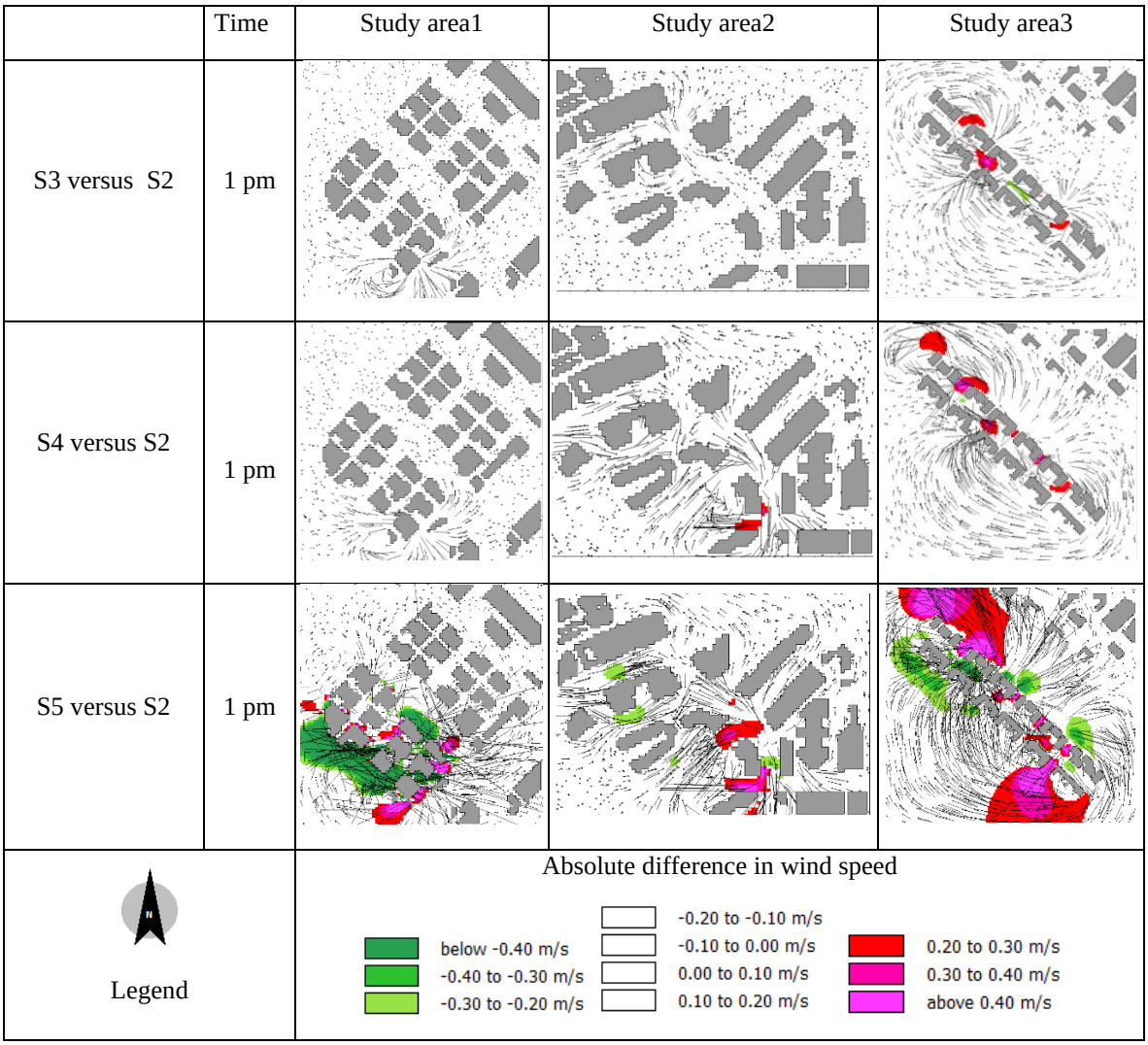

Fig. 16. Wind comparison of S3, S4, and S5 with S2 at 1 am and 1 pm in winter.

To present the wind ventilation results clearly and vividly, 3D views of the three study areas in S4 are presented as examples in Fig.17. This figure visualizes wind speed in the three study areas at the pedestrian level (1.5 m high), and also displays wind speed in a 3D view from the surface level to the building top level. The wind speed in open spaces in study areas 1, 2, and 3 is approximately 5 m/s to 6 m/s. At the top of certain open spaces, higher wind speeds (7 m/s to 8 m/s) are observed. When the wind reaches the buildings in these study areas, its speed decreases to approximately 1 m/s to 3 m/s at the street level because of friction force.

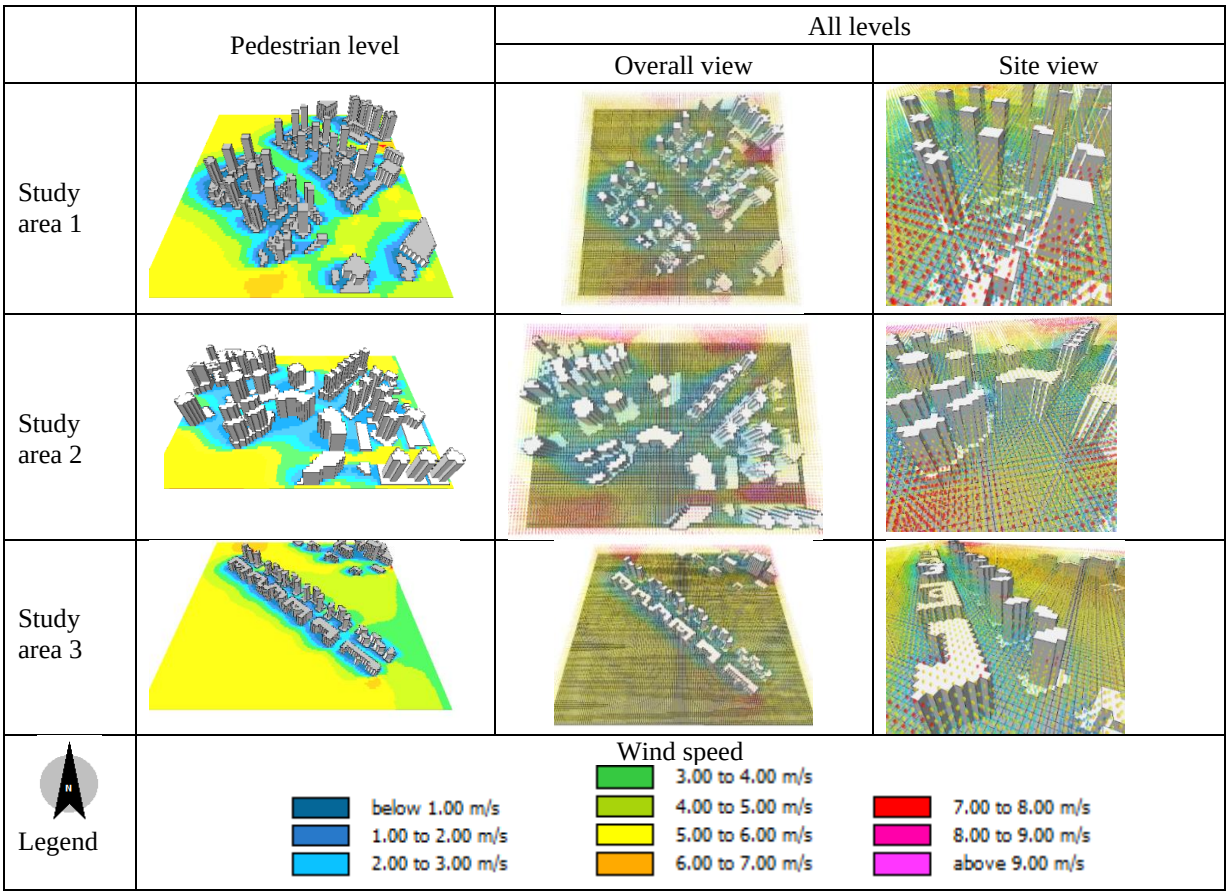

Fig. 17. Visualization of wind ventilation in the three study areas in S4 at 1 pm in winter.

5. Discussion and conclusions

5.1 Discussion

To probe the influences of minor relaxation of the maximum PR/BH restrictions of twenty-one study sites, 3D GIS, spatial analyses, and simulation technologies were applied. Only urban skyline, visibility, shadow and insolation, air temperature, and wind ventilation were considered, and the analyses of these factors were limited to the twenty-one target areas in this study. Therefore, spatial analyses related to urban heat island, transportation, drainage, public facilities, and other elements could be probed in a wider study region in future. The materials and color of architectures for 3D models could also be discussed in the further research.

A microclimate model consists of both cartographic information and meteorological configuration, and such a model can function as an example of the adaption of GIS in current real-life planning issues. The relationships between building height and meteorological data field within the study area could be analysed in future research by simulating the microclimate of the KTDA using a computational fluid dynamics-based model. As a pilot study focusing on the KTDA in Hong Kong, this research tentatively integrated 3D GIS spatial technology and control policy of urban development for the first time. The proposed approach can also be used in other urban renewal projects with a larger area, such as the Kowloon East Development in Hong Kong or similar areas in other densely populated cities.

Considering all kinds of influences, S4 is the recommended rational scale to relax the maximum PR/BH restriction for the twenty-one study sites because of the minor effect or slight changes. Compared to S2, additional GFA, residential units, and potential residents provided by S3 and S4 are shown in Table 5. The proposed relaxation of PR/BH will provide an additional 156,200 m^2 to the domestic GFA, and 119,900 m^2 to the non-domestic GFA in S4.

Table 5
Additional GFA, residential units, and potential residents provided by S3 and S4.

Scenario	Type	Area (m^2)	Plot ratio	Additional			
				Area (m^2)	Percent of area	Unit ($60m^2$/unit)	Residents (3.5person/unit)
2	Domestic	687,300	3.40-6.10	/	/	/	/
	Non-domestic	454,900	2.00-7.20	/	/	/	/
3	Domestic	766,300	3.60-6.80	79,000	11.4%	1,316	4,606
	Non-domestic	515,700	2.30-7.80	60,800	13.3%	/	/
4	Domestic	843,500	3.80-8.70	**156,200**	22.7%	2,603	9,110
	Non-domestic	574,800	2.30-8.50	**119,900**	26.4%	/	/

5.2 Conclusions

In this research, 3D GIS and simulation technologies were used to verify that to what extent the maximum PR/BH can be relaxed with only minor changes to the surrounding environment. 3D analysis and comparison of skyline, visibility, shadow and insolation, air temperature, and wind ventilation based on different five scenarios were successfully simulated and detected. The findings indicate that a minor relaxation of the PR/BH would lead to the following outcomes.

(1) After comparison, the influence of raising PR/BH on city skylines was negligible, which did not bring much visual changes to the residents and tourists.
(2) Sightlines were created through connecting the three vantage points in Hong Kong island to the sampling points on the limit roofline of the mountain to check the visibility on mountain ridgeline, which is an effective way to protect the urban ridgeline during urban redevelopment. For the continuously increasing PR/BH under the five scenarios, only one bundle of blocked sightlines appeared in S5 at the Quarry Bay Park vantage point. A very slight visual influence was noticed on the protection of mountain ridgelines and human visibility.
(3) For shadow and insolation analysis, the average sunlight hours per day, size of sunlight area, and the related percentages for various categories were computed both in summer and winter in the three study areas. The changes were insignificant in both summer and winter. The percentage of change in summer is a little larger than in winter, which is reasonable. The effect of shadow and insolation on the microenvironment and walkers was relatively small when PR/BH was increased.
(4) The effect of increasing PR/BH on air temperature was simulated successfully. Air temperature change in the three study areas was insignificant when the increase in PR/BH under all the scenarios was simulated in summer. The change was also insignificant in study areas 1 and 2 in winter when a proper increase in PR/BH was assumed (e.g. S3 and S4), while a slight decrease in air temperature was noted in study area 3 in S3 and S4 in winter's afternoon. When PR/BH was considerably increased in S5, the air temperature in

study areas 1 and 3 also changed significantly (approximately 0.2-0.4 °C changes) in winter. Fortunately, humans cannot feel air temperature changes within 1 °C.

(5) Wind ventilation showed an insignificant change in the three study areas under S3 and S4 in both winter and summer. In S5, a considerable change (0.2-0.4 m/s changes) in wind ventilation was observed in the three study areas in both winter and summer.

Finally, this study concludes that there is no significant impact on the skyline, visibility, and shadow and insolation under the five scenarios. The only significant changes occurred in air temperature and wind ventilation in the extreme case of S5. The findings demonstrate that the government and the public can evaluate the environmental influence of land development density from a holistic view, and make effective and farsighted decisions based on the 3D models and the results of spatial analysis. In addition, as a policy decision support tool for tapping the maximum potential of land use, the approach raised by this research can also be used to urban development or redevelopment cases in other high-density populated cities similar to Hong Kong.

Acknowledgements

This research was assisted through a grant from the Research Institute for Sustainable Urban Development (RISUD) of The Hong Kong Polytechnic University. The authors would like to thank the Building Healthy Kowloon City Association for its support.

References

Bottillo, S., Vollaro, A. D. L., Galli, G. and Vallati, A., 2014. CFD modeling of the impact of solar radiation in a tridimensional urban canyon at different wind conditions. Solar Energy, 102, 212–222.

Bourbia, F. and Awbi, H. B., 2004. Building cluster and shading in urban canyon for hot dry climate: Part 1: Air and surface temperature measurements. Renewable Energy, 29(2), 249–262.

Bradshaw, V., 2006. The building environment: active and passive control systems. John Wiley & Sons.

Building Department, 2012. Cap 123F Building (Planning) Regulations. https://www.google.com.hk/#safe=active&q=Building+(Planning)+Regulations.

Cai, X. M., 2012. Record Title: Effects of Wall Heating on Flow Characteristics in a Street Canyon. Boundary-Layer Meteorology, 142 (3), 443-467.

Chen, B., Huang, F. and Fang, Y., 2011. Integrating virtual environment and GIS for 3D virtual city development and urban planning, proceedings of 2011 IEEE International Geoscience and Remote Sensing Symposium, 24-29 July, Vancouver, Canada.

Civil Engineering and Development Department (CEDD), 2015. Broad Development Parameters of the Applied Use/Development in respect of Application No. A/K22/16. http://www.info.gov.hk/tpb/tc/plan_application/Attachment/20150303/s16_A_K22_16_0_gist.pdf.

Civil Engineering and Development Department (CEDD), 2008. Kai Tak Development. http://www.ktd.gov.hk/eng/overview.html.

Croker, B., 1956. Microclimate. Tuatara (Online), 6(2), 52. http://nzetc.victoria.ac.nz/tm/scholarly/tei-Bio06Tuat02-t1-body-d3.html.

Environmental Protection Department, 1997. Environmental Impact Assessment Ordinance. http://www.epd.gov.hk/eia/cindex.html.

Foth, M., Bajracharya, B., Brown, R. and Hearn, G., 2009. The second life of urban planning? Using neogeography tools for community engagement. Journal of Location Based Services, 3(2), 97-117.

Geertman, S., 2002. Participatory planning and GIS: A PSS to bridge the gap. Environmental and Planning B: Planning and Design, 29, 21-35.

Guo, J., Sun, B.X., Qin, Z., Wong, S.W., Wong, M.S., Yeung C.W., and Shen, Q.P., 2017. A study of plot ratio/building height restrictions in high density cities using 3D spatial analysis technology: A case in Hong Kong. Habitat International, 65(2017), 13-31.

Hong Kong Observatory (HKO), 2015. The Year's Weather-2015. https://www.hko.gov.hk/wxinfo/pastwx/2015/ywx2015.htm.
Hudson-Smith, A., Evans, S. and Batty, M., 2005. Building the virtual city – Public participation through e-Democracy. Knowledge, Technology, & Policy, 18(1), 62-85.
Insolation, 2018. https://simple.wikipedia.org/wiki/Insolation.
Isaacs, J. P., Gilmour, D. J., Blackwood, D. J. and Falconer, R. E., 2011. Immersive and non-immersive 3D virtual city: Decision support tool for urban sustainability. Journal of Information Technology in Construction, 16, 149-159.
Joardar, S. D., 1998. Carrying capacities and standards as bases towards urban infrastructure planning in India: a case of urban water supply and sanitation. Habitat International, 22(3), 327-337.
Johansson, E., 2006. Influence of urban geometry on outdoor thermal comfort in a hot dry climate: A study in Fez, Morocco. Building and Environment, 41(10), 1326-1338.
Kai Tak Development Urban Design Guidelines and Manual (KTDUDGM), 2015. http://www.ktd.gov.hk/udgm/en.
Maggiotto, G., Buccolieri, R., Santo, M. A., & Sabatino, S.D., 2014. Study of the urban heat island in Lecce (Italy) by means of ADMS and ENVI-ME. Int. J. Environ. Pollut., 55 (1/2/3/4), 41-49.
Mak, A. S.-H., Yip, E. K.-M. and Lai, P.-C., 2005. Developing a city skyline for Hong Kong using GIS and urban design guidelines. URISA Journal, 17(1), 33-42.
Maunsell AECOM., 2006. Kai Tak Development Engineering Study cum Design and Construction of Advance Works –Investigation, Design and Construction. Environmental Impact Assessment Report. http://www.epd.gov.hk/eia/register/report/eiareport/eia_1572008/.
Morakinyo, T. E. & Lam, Y. F., 2016. Simulation study on the impact of tree-configuration, planting pattern and wind condition on street-canyon's micro-climate and thermal comfort. Build. Environ., 103, 262-275.
Nakamura, Y. and Oke, T. R., 1988. Wind, temperature and stability conditions in an east-west oriented urban canyon. Atmospheric Environment, 22(12), 2691-2700.
Nations, U., 2014. World urbanization prospects: The 2014 revision, highlights. Department of economic and social affairs. Population Division, United Nations, 32.
Ng, E., Chen, L., Wang, Y., Yuan, C., 2012. A study on the cooling effects of greening in a high-density city: An experience from Hong Kong, Building and Environment, 47, 256-271. https://doi.org/10.1016/j.buildenv.2011.07.014.
Pettit, C. J., Cartwright, W. and Berry, M., 2006. Geographical visualization: A participatory planning support tool for imaging landscape futures. Applied GIS, 2(3), 1-17.
Planning Department, 2015. Urban Design Guidelines-Chapter 11.
Planning Department and RMUM Hong Kong Limited, 2002. Urban Design Guidelines for Hong Kong. http://www.pland.gov.hk/pland_en/p_study/comp_s/udg/udg_es/udg_es_eng.pdf.
Pullar, D. V. and Tidey, M. E., 2001. Coupling 3D visualization to qualitative assessment of built environment designs. Landscape and Urban Planning, 55, 29-40.
Ranzinger, M. and Gleixner, G., 1997. GIS Datasets for 3D urban planning. Comput., Environ. and Urban Systems, 21(2), 159-173.
Shadow, 2019. https://en.wikipedia.org/wiki/Shadow.
Shahidan, M. F., Jones, P. J., Gwilliam, J., Salleh, E., 2012. An evaluation of outdoor and building environment cooling achieved through combination modification of trees with ground materials, Building and Environment, 58, 245-257. https://doi.org/10.1016/j.buildenv.2012.07.012.
Shen, Q.P., Chen, Q., Tang, B.S., Yeung, S., Hu, Y.C. and Cheung G., 2009. A system dynamics model for the susta inable land use planning and development. Habitat International, 33, 15–25.
Stevens, D., Dragicevic, S. and Rothley, K., 2007. iCity: A GIS - CA modelling tool for urban planning and decision making. Environmental Modelling & Software, 22, 761-773.
Town Planning Board (TPB), 2012. Outline Zoning Plans, Kowloon Planning Area NO.22 Approved Kai Tak Outline Zoning Plan No. S/K22/4.
Town Planning Board (TPB), 2015. Statutory Planning Portal 2. http://www2.ozp.tpb.gov.hk/gos/default.aspx.
Wang, Y., Zhong, K., Zhang, N. and Kang, Y., 2013. Numerical Analysis of Solar Radiation Effects on Flow Patterns in Street Canyons. Engineering Applications of Computational Fluid Mechanics, 8(2), 252-262.
Wong, M. S, Nichol, J. and Ng, E., 2011. A study of the "wall effect" caused by proliferation of high-rise buildings using GIS techniques. Landscape and Urban Planning, 102, 245-253.
Xu, Z. and Coors, V., 2012. Combining system dynamics model, GIS and 3D visualization in sustainability assessment of urban residential development. Building and Environment, 47, 272-287.

Xun, P., Huang, S., & Chen, Z., 2014. Improvement strategy for outdoor environment quality in commercial street based on ENVI-met simulation. Appl. Mech. Mater., 641-642, 1131-1136.

Yeo, I.-A., Yoon, S.-H. and Yee, J.-J., 2013. Development of an environment and energy geographical information system (E-GIS) construction model to support environmentally friendly urban planning. Applied Energy, 104, 723-739.

Zhang, X., Zhu, Q. and Wang, J. W., 2004. 3D city models based spatial analysis to urban design. Geographic Information Sciences, 10(1), 82-86.